RNPS1 in PSAP complex controls cyclical pre-mRNA splicing over the cell cycle

Kazuhiro Fukumura[1,*], Akio Masuda[2], Jun-ichi Takeda[2], Kinji Ohno[2] and Akila Mayeda[1,*]

[1]Division of Gene Expression Mechanism, Center for Medical Science, Fujita Health University, Toyoake, Aichi 470-1192, Japan
[2]Division of Neurogenetics, Center for Neurological Disease and Cancer, Nagoya University Graduate School of Medicine, Nagoya, Aichi 466-8550, Japan

*To whom Correspondences should be addressed. Tel: +81 562 93 9378; Email: fukumura@fujita-hu.ac.jp (K.F.). Tel: +81 562 93 9377; Email: mayeda@fujita-hu.ac.jp (A.M.)

Keywords: Pre-mRNA splicing, periodic splicing, cell cycle, *AURKB* gene, RNPS1, PNN (PININ), SAP18, PSAP complex

ABSTRACT

Cell cycle progression must require periodic gene expression through the control of splicing. However, the splicing factors that directly control this cell cycle-dependent splicing remain unknown. Cell cycle-dependent expression of the *AURKB* (aurora kinase B) gene is essential for chromosome segregation and cytokinesis and we previously reported that RNPS1 is essential to maintain precise splicing in *AURKB* intron 5. Here we show that RNPS1 plays this role in PSAP complex with PNN (PININ) and SAP18, but not in ASAP complex with ACIN1 (ACINUS) and SAP18. A transcriptome-wide analysis of RNPS1- and PNN-deficient cells indicated that the PSAP complex globally controls pre-mRNA splicing during cell cycle progression. Remarkably, protein expression of RNPS1, but not PNN, is cell cycle-dependently coordinated with splicing in PSAP-controlled introns, including *AURKB* intron 5, implicating RNPS1 as a key factor controlling periodic splicing during the cell cycle.

GRAPHICAL ABSTRACT

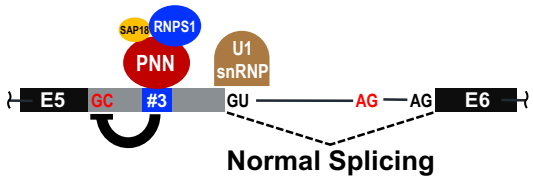

RNPS1 in PSAP Maintains Precise Splicing

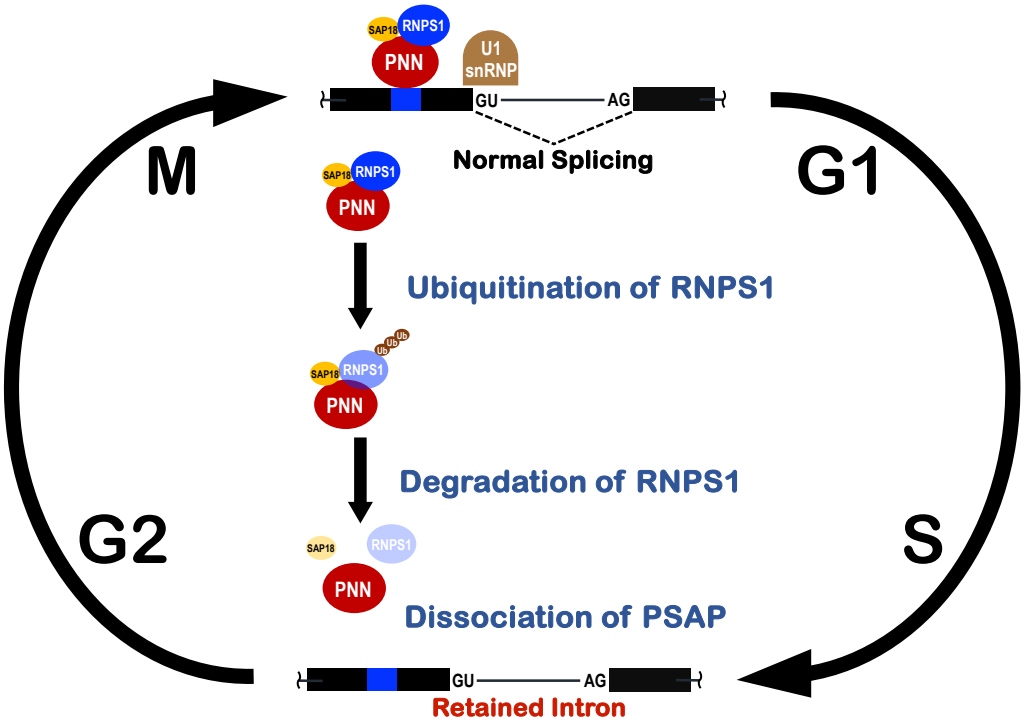

RNPS1 in PSAP Controls Cell Cycle-Dependent Splicing

INTRODUCTION

Human pre-mRNA splicing takes place in the huge multimolecular complex, termed spliceosome, that is a highly organized dynamic ribonucleoprotein machine comprised of five snRNPs and numerous proteins (reviewed in 1,2). Amidst the panoply of proteins in this spliceosome, it is amazing to observe that individual protein factors often drastically change the outcome of splicing in a precisely regulated manner.

We originally identified human RNPS1 (RNA binding protein with serine-rich domain 1) as a general splicing activator *in vitro* (3). We found that RNPS1 interacts with the spliceosome and regulates a variety of alternative splicing events, often collaborating with other splicing regulators, such as SRSF11 (p54), TRA2B (hTra2β), and PNN (PININ) (4,5). RNPS1 was also identified as a peripheral factor of the exon junction complex (EJC) (reviewed in 6,7).

ACIN1 (ACINUS) and PNN are scaffold proteins and form two alternative ternary complexes with RNPS1 and SAP18, termed ASAP and PSAP, respectively (8,9). ACIN1 is involved in apoptosis and regulation of splicing and transcription (10-12) and PNN was originally identified as a desmosome-associated protein but also function as a regulator of alternative splicing (13,14).

Since ACIN1 bridges the ASAP complex to the EJC core (14) and PNN can be structurally replaced with ACIN1 to form PSAP (9), both ASAP and PSAP whole complexes must interact with the EJC. Recent transcriptome-wide analysis indicated that the ASAP and PSAP complexes regulate distinct alternative splicing either in EJC core-dependent or -independent manner (14). On the other hand, the EJC core alone, without any peripheral factors, plays a role in terminating splicing; i.e., repression of aberrant re-splicing on mature mRNA in cancer cells (15). Many lines of evidence support ASAP and PSAP complexes, with or without EJC core, as regulators of alternative splicing (reviewed in 7). However, their biological and physiological significance remains to be investigated.

We have been studying splicing regulation involved in mitotic cell-cycle progression using the *AURKB* (aurora kinase B) gene as a model. The *AURKB* gene encodes a serine/threonine protein kinase that is essential in chromosome segregation and cytokinesis during the cell cycle (reviewed in 16). We previously showed that RNPS1, recruited by the EJC core, is critical for efficient and faithful splicing in mitotic cell cycle-related genes including *AURKB* (17). Indeed, RNPS1 depletion causes a reduction of the AURKB protein due to multiple aberrant splicing, resulting in abnormal multinucleation phenotype that is rescued by ectopic expression of AURKB (18). Regarding the mechanism of action, we found that RNPS1 protein binds directly to a specific element in exon 5 upstream of the authentic 5′ splice site, and this binding is required to repress multiple aberrant splicing using a common pseudo 5′ splice site (18). Here we showed that RNPS1 plays a role as the PSAP component in preventing aberrant splicing of *AURKB* pre-mRNA.

It was reported that SR protein kinase CLK1 (CDC-like kinase 1) controls many periodically spliced pre-mRNAs, including *AURKB*, during the cell cycle (19). However, splicing factors were not known to be directly involved in cyclical splicing. Here we have discovered that the protein level of RNPS1 is coordinated with cell cycle-dependent periodic splicing of *AURKB* pre-mRNA. We propose a novel function of RNPS1 in PSAP complex, as a critical modulator that temporally controls periodic splicing observed during cell cycle.

MATERIALS AND METHODS

Construction of expression plasmids

The pcDNA3-Flag-RNPS1 expression plasmid was described previously (18). To construct the expression plasmids, pcDNA3-AURKB/E5-WT and the pcDNA3-AURKB/E5-Δ#3, the fragments containing the 3′ end of intron 4, exon 5 and the 5′ end of intron 5 were amplified by PCR from pcDNA3-AURKB/E5-E6 and pcDNA3-AURKB/E5-E6-Δ#3 plasmids (18), respectively, and these were subcloned into pcDNA3 vector (Invitrogen–Thermo Fisher Scientific). The pcDNA3-AURKB/E5/inR-E6 and pcDNA3-AURKB/E5/inL-E6 plasmids were constructed using overlap extension PCR as previously described (20). All PCRs were performed with PrimeSTAR Max DNA Polymerase (Takara Bio) using the described primer sets (Supplementary Table S1).

RNAi-mediated knockdown and splicing assays

HeLa cells and HEK293 cells (in 35-mm dishes) were grown at 37°C under 5% CO_2 in Dulbecco's modified Eagle's medium (DMEM; Wako) supplemented with 10% fetal bovine serum (FBS) and 1% penicillin-streptomycin (Nakarai Tesque). The transfection of cells with siRNAs (100 pmol each) was performed using Lipofectamine RNAi max (Invitrogen-Thermo Fisher Scientific) according to manufacturer's protocol. The siRNAs targeting RNPS1, ACIN1, PNN, SAP18, GPATCH8 and LUC7L3 (Supplementary Table S1) were purchased (Nippon Gene).

At 72 h post-transfection, total RNAs were isolated from HeLa and HEK293 cells using the NucleoSpin RNA kit (Macherey-Nagel). To examine endogenous mRNA expression levels and the splicing products, total RNAs were reverse transcribed using PrimeScript II reverse transcriptase (Takara Bio) with oligo-dT and random primers, and the obtained cDNAs were analyzed by PCR and quantitative PCR (qPCR) using specific primer sets (Supplementary Table S1).

All primers oligonucleotides were purchased (Fasmac) and all PCRs were performed with Blend Taq polymerase (Toyobo). The PCR products were analyzed by 6% polyacrylamide gel electrophoresis (PAGE). PCR products of aberrantly spliced and intron retained mRNAs were quantified using NIH Image J software. Eco Real-Time PCR system (Illumina) was used for qPCR analysis with Thunderbird SYBR qPCR Mix (Toyobo). All the experiments were independently repeated three times. Mean values, standard error of the mean (SEM), and Welch's *t*-test were calculated using Excel (Microsoft).

Western blotting analysis

At 72 h post-transfection, total protein was isolated from siRNA-treated HeLa and HEK293 cells to examine the endogenous protein expression levels. Cells were suspended in Buffer D [20 mM HEPES (pH 7.9), 50 mM KCl, 0.2 mM EDTA, 20% glycerol], sonicated for 20 sec, centrifuged to remove debris, and the lysates were subjected to Western blotting. The procedure, detection and analysis were described previously (20). The following antibodies were used to detect target proteins: anti-RNPS1 (1:750 dilution, 3), anti-ACIN1 (1:1500 dilution; Cells Signaling Technology), anti-PNN (1:1500

dilution; Sigma-Aldrich), anti-SAP18 (1:1500 dilution; Proteintech), anti-AURKB (1:1500 dilution; Cells Signaling Technology) and anti-GAPDH (1:1500 dilution; MBL Life Science) antibodies.

RNA immunoprecipitation assay

HeLa cells (in 60-mm dishes) were co-transfected with pcDNA3-Flag-RNPS1 and pcDNA3-AURKB/E5-WT or the pcDNA3-AURKB/E5-Δ#3 using Lipofectamine 2000 (Invitrogen–Thermo Fisher Scientific). After culturing for 48 h, whole cell extracts were prepared and mixed with each antibody conjugated with Dynabeads Protein A (Invitrogen–Thermo Fisher Scientific). After culturing for 48 h, whole cell extracts were prepared and mixed with each antibody) in NET2 buffer [50 mM Tris (pH 7.5), 150 mM NaCl, 0.05% Nonidet P-40]. After 3 h incubation at 4°C, the beads were washed six times with NET2 buffer and bound RNA was eluted by TRI Reagent (Molecular Research Center). The precipitated RNAs were reverse transcribed by PrimeScript II reverse transcriptase (Takara Bio) with oligo-dT primers, and the cDNAs were detected by PCR using the specific primer sets (Supplementary Table S1). The PCR products were analyzed by 2% agarose gel.

RNA-Seq and gene ontology analyses

The RNA libraries were prepared from three RNA sources; HEK293 cells transfected with siRNAs targeting RNPS1 and PNN (with control siRNA). mRNA isolation, cDNA library construction and whole-transcriptome sequencing was performed by Macrogen Japan Corporation. The obtained reads were mapped to the human genome as follows. FASTQ files were filtered by Trimmomatic v0.36 (21) with the parameters "PE -phred33 ILLUMINACLIP:Trimmomatic-0.36/adapters/TruSeq3-PE.fa:2:30:10 LEADING:3 TRAILING:3 SLIDINGWINDOW:4:15 MINLEN:150" and trimmed by fastx_trimmer included in the FASTX-Toolkit v0.0.13 (http://hannonlab.cshl.edu/fastx_toolkit/index.html) with the parameter "-l 150". The qualified FASTQ files were mapped to human genome hg19 by TopHat v2.1.1 (22) and the transcripts were assembled by Cufflinks v2.2.1 (23) with default parameters. PSI (percent-spliced-in) values were estimated by MISO v0.5.2 (24) using the assembled transcripts as previously described (25).

A gene ontology database, DAVID Bioinfomatics Resources (version 6.8; https://david.ncifcrf.gov/), was used to identify functional annotation of the genes that are significantly enriched in a particular function. The obtained list of gene symbols of PSAP regulated alternative splicing events were used as input for DAVID analysis. DAVID calculates a modified Fisher Extract *p*-value. We set a count threshold of 2 and the default value of 0.1 for the enrichment score (EASE).

Cell cycle synchronization experiments

To achieve cell synchronization at G2/M phase, HEK293 cells were plated (in 35-mm dishes) at 40% confluency. Cells were subsequently treated with 2 mM thymidine (Sigma-Aldrich) for 24 h, washed with PBS, and supplemented with fresh DMEM. After culture for 3 h, cells were followed by 12 h culture in the presence of microtubule-disrupting agent nocodazole at 100 μM concentration (Sigma-

Aldrich). To remove nocodazole, cells were washed with phosphate-buffered saline (PBS) and cultured in fresh DMEM. Cells were harvested every 4 h for 12 h after the removal of nocodazole.

To achieve cell synchronization at G1/S phase, HEK293 cells were plated (in 35 mm dishes) at 20% confluency. Cells were treated with 2 mM thymidine for 18 h, washed with PBS, and supplemented with DMEM. After culture for 9 h, cells were treated with 2 mM thymidine for another 15 h. Cells were released from thymidine block by washing with PBS followed by culture in fresh DMEM. Cells were harvested every 4 h for 12 h after the removal of thymidine.

To inhibit proteasome, HEK293 cells were treated with MG132 (Sigma-Aldrich) at a final concentration of 1 or 10 μM. After 16 h of culture, cells were harvested and total protein was isolated (see above).

RESULTS

PSAP promotes efficient and precise splicing of *AURKB* pre-mRNA

Previously, we reported that RNAi-mediated knockdown of RNPS1 induced aberrant splicing in the *AURKB* intron 5 and *MDM2* intron 10 (Supplementary Figure S1A), and we identified the functional RNPS1 binding site upstream of the *AURKB* intron 5 (18). On the other hand, our previous yeast two-hybrid screening revealed that RNPS1 can bind to ACIN1, PNN, GPATCH8 and LUC7L3 (4). This observation is consistent with the later finding that ACIN1 and PNN form the ASAP and PSAP complex, respectively, with the common components RNPS1 and SAP18.

We then performed knockdown of all the components of the PSAP and ASAP complexes; i.e., RNPS1, ACIN1, PNN and SAP18. We confirmed that each siRNA led to effective depletion of the target mRNA and the protein product (Figure 1A). Notably, the knockdown of RNPS1, ACIN1 and PNN also caused co-depletion of SAP18 protein, however SAP18 mRNA levels were barely changed, indicating that SAP18 protein is stabilized in either ASAP or PSAP complex. Then, we examined whether these PSAP- and ASAP-components operate together with RNPS1 to ensure precise splicing in the *AURKB* intron 5 (Figure 1B) and the *MDM2* intron 10 (Supplementary Figure S1B). We found that the knockdown of PNN and SAP18, as well as RNPS1, induced intron retention and aberrant splicing at expense of normal mRNA, but knockdown of ACIN1 did not. This confirms that the PSAP, but not ASAP, plays a role to restore the normal splicing in *AURKB* intron 5. The knockdown of other RNPS1-binding proteins, GPATCH8 and LUC7L3, have no effects on normal splicing (I) in the *AURKB* intron 5 and *MDM2* intron 10 (Supplementary Figure S1B).

Previously, we demonstrated that RNPS1 binds to a specific *cis*-acting element (termed #3) located upstream of the authentic 5′ splice site of intron 5 (Figure 1C, upper scheme) (18). We thus examined whether the PSAP complex binds to this *cis*-acting element. We transfected HEK293 cells with the AURKB/E5-WT or AURKB/E5-Δ#3 reporter mini-genes and performed RNA immunoprecipitation experiments using antibodies against each of the PSAP components (Figure 1C, lower panel). As we expected, RNPS1, PNN and SAP18 bound to the AURKB/E5-WT, but ACIN1 did not. Notably, deletion of this *cis*-acting element '#3' greatly reduced the binding of the PSAP components. We conclude that PSAP binding to the specific element '#3' is critical for efficient and precise splicing in the *AURKB* intron 5.

PSAP represses the *AURKB* pseudo 5′ splice site without steric hindrance

Since the '#3' element is located between the upstream pseudo 5′ splice site and the downstream authentic 5′ splice site, we postulated two conceivable mechanisms of activation or de-repression: (i) PSAP interacts with the U1 snRNP to activate the authentic 5′ splice site, and/or (ii) PSAP binding causes steric hindrance and masks the adjacent pseudo 5′ splice site (Figure 2A). We examined these two possibilities by increasing the distance of the '#3' element from either the authentic 5′ splice site or the pseudo 5′ splice site (Figure 2B).

These two variant *AURKB* pre-mRNAs, as well as the original *AURKB* pre-mRNAs, had equivalent repression of the normal 5′ splice site by the RNPS1-knockdown (Figure 2C), suggesting that neither postulated mechanism (see above) is the case. In endogenous *AURKB* pre-mRNA, RNPS1-knockdown produces five aberrant mRNAs using a common upstream pseudo 5′ splice site that is much stronger than the downstream normal 5′ splice site (18). Therefore, the most plausible mechanism is repression of the pseudo 5' splice site triggered by the PSAP binding, however, direct masking of the pseudo 5' splice site is unlikely.

PSAP globally modulates alternative splicing involved in cell cycle progression

To test whether PSAP might have a general role in controlling splicing, we performed whole-transcriptome sequencing (RNA-Seq) analysis in the RNPS1- and PNN-deficient HEK293 cells. The sequencing reads were mapped to the human genome sequences and we analyzed splicing changes in five major classes; i.e., cassette exon, alternative 5′ splice site, alternative 3′ splice site, mutually exclusive exons, and intron retention (Supplementary Tables S2 and S3). We identified a total of 289 overlapping splicing changes in the RNPS1- and PNN-deficient HEK293 cells, and the most frequent class of the overlapping events (131/289) was intron retention, or splicing defect (Figure 3A, Supplementary Table S4).

We also analyzed the biological functions of the corresponding genes in which the 289 splicing events were controlled by PSAP. Remarkably, we noticed that the most enriched functional category was the mitotic cell cycle, and cell cycle-related categories appeared in the top list, including regulations of mitotic cell cycle and cell cycle process (Figure 3B). These data implicate PSAP as a global controller of splicing involved in cell cycle progression.

RNPS1 in PSAP controls periodic splicing in the cell cycle

A previous RNA-Seq analysis at different stages of the cell cycle identified ~1300 genes with changes of cell cycle-dependent alternative splicing, and interestingly, the intron retention event of *AURKB* intron 5 was characterized as a representative model (19). The excision of *AURKB* intron 5 was periodically modulated and this splicing activity reaches the maximum around M phase (Figure 4A). Since our gene ontology analysis suggested that PSAP regulates the alternative splicing of a set of genes involved in mitotic cell cycle progression, we hypothesized that PSAP controls cell cycle-dependent splicing.

We first recapitulated the periodic splicing of *AURKB* intron 5 during cell cycle progression with HEK293 cells (Figure 4B). We then treated the cells with the microtubule-destabilizing reagent, nocodazole, which arrests cells cycle at the start of the G2/M phase (nocodazole release 0 h). Using RT–PCR and quantitative RT–PCR (RT–qPCR), we observed increased intron 5 retention from G2/M to G1/S phase (nocodazole release 4–8 h). On the other hand, we found decreasing intron 5 retention from G1/S to G2/M phase in synchronized HEK293 cells after release from the double thymidine block at the G1/S boundary (Supplementary Figure S2).

It was important to confirm whether the observed cyclical splicing modulation is a general event in all the PSAP-controlled introns. We thus tested three representative PSAP-controlled introns, *ADCK4* intron 6, *VPS13D* intron 44 and *HERC2* intron 61 (arbitrarily chosen from Supplementary Table S4). Intron retention was observed in PSAP components (RNPS1 and PNN)-deficient cells, and not in the control *ACTG1* intron 3 (Figure 5A). Then, we examined the changes in intron retention events during the cell cycle using nocodazole and double thymidine to synchronize HEK293 cells (Figure 5B, Supplementary Figure S2). Remarkably, in these PSAP-controlled introns, we also observed periodic changes in the intron retention as observed in *AURKB* intron 5 pre-mRNA (Figure 4B, Supplementary Figure S2). Our experimental observations thus provided the mechanistic basis to the reported periodical pattern of splicing activity (Figure 4A). Taken together, we propose that PSAP promotes periodic splicing linked to the cell cycle.

Periodic change of RNPS1 protein is mediated by the proteasome/ubiquitin system

We assumed that PSAP-controlled periodic splicing was modulated by the expression level changes of PSAP components. We thus examined the protein levels of PSAP components during the cell cycle using nocodazole synchronized HEK293 cell (Figure 6A, left panel). Intriguingly, RNPS1 protein level was at a maximum in G2/M phase (nocodazole release 0 h) and decreased through cell cycle progression (nocodazole release 4–8 h), and then started to increase again (nocodazole release 12 h). This periodic change in RNPS1 protein was coordinated with the level of AURKB protein, which was at a high level in G2/M and declined to a low level in G1/S by degradation (Figure 6A, left panel) (26). In contrast, protein levels of other PSAP components PNN and SAP18, as well as an ASAP component ACIN1, were barely changed. Notably, we did not observe such a periodic change in RNPS1 mRNA expression level during cell cycle (Figure 6A, right graph) as previously observed in human RNPS1 (E5.1) (27). These data together indicate that the reduction of RNPS1 protein level is regulated at the protein level, but not at the mRNA level.

We also performed the same experiments using the double thymidine block synchronized HEK293 cells (Figure 6B, left panel). We found that RNPS1 protein was minimum at G1/S phase (double thymidine release 0 h) and increased as the cell cycle progressed to G2/M phase (double thymidine block 4–12 h). The protein expression of ACIN1, PNN, and SAP18 were also somewhat increased. These results could be partly due to the mRNA level of PSAP components, RNPS1 and PNN, that together with AURKB, were increased from G1/S into G2/M phase (Figure 6B, right graph).

Since RNPS1 and AURKB protein expressions were synchronized during the cell cycle (Figure 6A, B, left panels), we assumed that RNPS1, but not other PSAP components, was responsible for the observed cell cycle-dependent splicing modulation (Figure 4B, D; Supplementary Figure S2). To test

this assumption, we performed nocodazole treatment in RNPS1-knockdown HEK293 cell and analyzed intron retention events in the PSAP-controlled introns. We found that RNPS1-knockdown induced the intron retention even at the RNPS1-upregulated G2/M phase (Supplementary Figure S3). We conclude that RNPS1, as a component of the PSAP, promotes the periodic pre-mRNA splicing linked to cell cycle progression.

Ubiquitin-mediated proteolysis is one of the keys to cell cycle progression (28). RNPS1 is polyubiquitinated by K48-linkage and degraded by the proteasome (29). Therefore, we assume that periodical degradation of RNPS1 protein is controlled by ubiquitin-proteasome pathway. We treated HEK293 cells with proteasome inhibitor MG132 and we examined the protein level of PSAP components. As we expected, RNPS1 protein was stabilized in the presence of MG132 whereas the level of other ASAP/PSAP proteins, ACIN1, PNN and SAP18, were not changed at all (Figure 6C). Taken together, we conclude that ubiquitin-proteasome system plays a critical role in the periodic fluctuation of RNPS1 protein level, leading to eventual splicing modulation in accordance with the cell cycle (Figure 7).

DISCUSSION

The PSAP complex is critical to maintain splicing fidelity

We previously reported that RNPS1 interacts with a specific *cis*-element and ensures precise splicing in the *AURKB* pre-mRNA, which is essential for chromosome segregation and cytokinesis (18). Here, we found that RNPS1 is accompanied by PNN and SAP18 to precisely splice out *AURKB* intron 5, and all these PSAP components bind to the same *cis*-element in the upstream exon (Graphical Abstract, upper panel).

The PSAP components (PNN, SAP18 and RNPS1) are all associate with the EJC core as peripheral factors (reviewed in 6,7). Therefore, it is conceivable that the EJC recruits the PSAP complex on the target pre-mRNA and PSAP itself functions to repress aberrant splicing. Indeed, we found that EJC core on pre-mRNA promotes splicing involved in mitotic cell cycle with RNPS1 as a key factor (17).

Regarding the mechanism of PSAP-mediated splicing correction in *AURKB* pre-mRNA, our data implicate that it occurs through repression of the pseudo 5' splice site without direct masking, rather than activation of the normal 5' splice site. Two recent observations that EJC-recruited PSAP represses distant pseudo and recursive 5′ splice site suggesting shared mechanism (30,31), however, the underlying mechanism of action remains uncertain.

A novel RNPS1 function in periodical splicing during the cell cycle

Cyclical removal of *AURKB* intron 5 contributes to periodic AURKB protein expression during the mitotic cell cycle (19); however, the molecular mechanism remains to be elucidated. Our finding provides a breakthrough in addressing this intriguing open question. Here we propose that splicing activator RNPS1 in PSAP complex not only functions to ensure precise splicing, but also plays an essential role in controlling periodic splicing linked to cell cycle (Graphical Abstract, lower panel).

Our whole-transcriptome sequencing (RNA-Seq) analysis in RNPS1- and PNN-knockdown cells showed that most affected splicing events were intron retentions, and our arbitrarily chosen intron retention events were all induced from G2/M phase to G1/S phase as observed previously in *AURKB* intron 5 (19). Notably, the gene ontology analysis revealed that splicing changes caused by PSAP-depletion often occur in genes involved in the mitotic cell cycle. We eventually discovered that the protein level of RNPS1 is down regulated in G1/S phase by the ubiquitin proteasome pathway and it gradually increases up to its maximum level at M phase. This characteristic temporal fluctuation of the RNPS1 protein level is well accounted for by the periodic splicing in accordance with the cell cycle (Figure 7). Since the protein levels of other PSAP components, PNN and SAP18, remain constant during the cell cycle, it is likely that the functional PSAP complex is dissociated by the lack of RNPS1 component.

Previously, it was reported that knockdown of EJC-core component, RBM8A (Y14), induces abnormal nuclear structure, multinucleated cells, G2/M cell cycle arrest, and genome instability (17,32; and references therein), which is a similar phenotype to that caused by the knockdown of PSAP component, RNPS1 (18). In mouse models, it was reported that haploinsufficiency of MAGOH, the other EJC core component, causes the defect of mitosis of neural stem cells, ending up in microcephaly (33). Together, it is very likely that the EJC recruits the functional PSAP complex on the cell cycle-dependently spliced pre-mRNAs, as well as on the pre-mRNAs to ensure splicing fidelity.

We demonstrate that PSAP, but not ASAP, controls the faithful splicing and alternative splicing of transcripts involved in the mitotic cell cycle. Therefore, the function of these two complexes is determined by only one distinct component of PSAP and ASAP, i.e., PNN and ACIN1 (Figure 1A, top schemes). Consistently, a recent report showed that PSAP and ASAP form functionally distinct complexes with the EJC core to confer distinct alternative splicing activities (14). On the other hand, since RNPS1 is a common component of PSAP and ASAP, periodic changes of RNPS1 protein would also be expected to modulate the function of ASAP during the cell cycle. Indeed, a possible function of ASAP in the cell cycle is suggested by the fact that depletion of the component of ASAP, ACIN1, cause defects in cell cycle progression (34). Moreover, the genome-wide identification of RNA targets suggests the role of ACIN1 in cell cycle (12). Taken together, we speculate that PSAP and ASAP complexes may target distinct subsets of pre-mRNAs and control periodic changes of splicing during the cell cycle.

DATA AVAILABILITY

The raw data derived from RNA-Seq analysis (see Figure 3A) have been deposited in DDBJ database under accession number DRA016802.

SUPPLEMENTARY DATA

Supplementary Data are available in the separate file.

ACKNOWLEDGEMENTS

We thank H. Shirasaki and T. Kanehisa for technical support; and members of our labs for constructive discussions. Author contributions were as follows: K. Fukumura and A. Mayeda conceived and designed the experiments; K. Fukumura performed most of the experiments and analyses, organized the data and drafted the manuscript; J.-i. Takeda and A. Masuda performed bioinformatics analyses of the sequencing data; K. Fukumura, K. Ohno and A. Mayeda revised and edited the manuscript. A. Mayeda coordinated and supervised the whole project. All authors read, corrected and approved the final manuscript.

FUNDING

K. Fukumura was partly supported by Grants-in-Aid for Scientific Research (C) [Grant numbers: 18K07304, 21K07202] from the Japan Society for the Promotion of Science (JSPS), a Research Grant from the Hori Sciences and Arts Foundation, and a Research Grant from Nitto Foundation, a Research Grant from Takeda Science foundation, and a Research Grant from Aichi Cancer Research Foundation. A. Masuda was partly supported by Grants-in-Aid for Scientific Research (B) [Grant numbers: JP21H02476, JP21H02838], Grant-in-Aid for Challenging Research (Exploratory) [Grant number: JP22K19269] from JSPS, and a Grant from the Japan Agency for Medical Research and Development [Grant number: JP23ek0109497]. K. Ohno was partly supported by Grants-in-Aid for Scientific Research (B) [Grant number: JP23H02794] from JSPS and Health and Labour Science Research Grant [Grant number: 23FC1014] from the Ministry of Health Labour and Welfare. A. Mayeda was partly supported by Grants-in-Aid for Scientific Research (B) [Grant number: JP16H04705] and Grants-in-Aid for Scientific Research (C) [Grant number: JP21K06024] from JSPS.

REFERENCES

1. Will, C.L. and Lührmann, R. (2011) Spliceosome structure and function. *Cold Spring Harb. Perspect Biol.*, **3**, a003707.

2. Kastner, B., Will, C.L., Stark, H. and Lührmann, R. (2019) Structural Insights into Nuclear pre-mRNA Splicing in Higher Eukaryotes. *Cold Spring Harb. Perspect. Biol.*, **11**, a032417.

3. Mayeda, A., Badolato, J., Kobayashi, R., Zhang, M.Q., Gardiner, E.M. and Krainer, A.R. (1999) Purification and characterization of human RNPS1: a general activator of pre-mRNA splicing. *EMBO J.*, **18**, 4560–4570.

4. Sakashita, E., Tatsumi, S., Werner, D., Endo, H. and Mayeda, A. (2004) Human RNPS1 and its associated factors: a versatile alternative pre-mRNA splicing regulator in vivo. *Mol. Cell. Biol.*, **24**, 1174–1187.

5. Trembley, J.H., Tatsumi, S., Sakashita, E., Loyer, P., Slaughter, C.A., Suzuki, H., Endo, H., Kidd, V.J. and Mayeda, A. (2005) Activation of pre-mRNA splicing by human RNPS1 is regulated by CK2 phosphorylation. *Mol. Cell. Biol.*, **25**, 1446–1457.

6. Le Hir, H., Sauliere, J. and Wang, Z. (2016) The exon junction complex as a node of post-transcriptional networks. *Nat. Rev. Mol. Cell Biol.*, **17**, 41–54.

7. Schlautmann, L.P. and Gehring, N.H. (2020) A Day in the Life of the Exon Junction Complex. *Biomolecules*, **10**, 866.

8. Schwerk, C., Prasad, J., Degenhardt, K., Erdjument-Bromage, H., White, E., Tempst, P., Kidd, V.J., Manley, J.L., Lahti, J.M. and Reinberg, D. (2003) ASAP, a novel protein complex involved in RNA processing and apoptosis. *Mol. Cell. Biol.*, **23**, 2981–2990.

9. Murachelli, A.G., Ebert, J., Basquin, C., Le Hir, H. and Conti, E. (2012) The structure of the ASAP core complex reveals the existence of a Pinin-containing PSAP complex. *Nat. Struct. Mol. Biol.*, **19**, 378–386.

10. Joselin, A.P., Schulze-Osthoff, K. and Schwerk, C. (2006) Loss of Acinus inhibits oligonucleosomal DNA fragmentation but not chromatin condensation during apoptosis. *J. Biol. Chem.*, **281**, 12475–12484.

11. Barrett, S.P., Wang, P.L. and Salzman, J. (2015) Circular RNA biogenesis can proceed through an exon-containing lariat precursor. *Elife*, **4**, e07540.

12. Rodor, J., Pan, Q., Blencowe, B.J., Eyras, E. and Caceres, J.F. (2016) The RNA-binding profile of Acinus, a peripheral component of the exon junction complex, reveals its role in splicing regulation. *RNA*, **22**, 1411–1426.

13. Wang, P., Lou, P.J., Leu, S. and Ouyang, P. (2002) Modulation of alternative pre-mRNA splicing in vivo by pinin. *Biochem. Biophys. Res. Commun.*, **294**, 448–455.

14. Wang, Z., Ballut, L., Barbosa, I. and Le Hir, H. (2018) Exon Junction Complexes can have distinct functional flavours to regulate specific splicing events. *Scientific reports*, **8**, 9509.

15. Otani, Y., Fujita, K.I., Kameyama, T. and Mayeda, A. (2021) The Exon Junction Complex Core Represses Cancer-Specific Mature mRNA Re-splicing: A Potential Key Role in Terminating Splicing. *Int. J. Mol. Sci.*, **22**, 6519.

16. Krenn, V. and Musacchio, A. (2015) The Aurora B kinase in chromosome bi-orientation and spindle checkpoint signaling. *Front. Oncol.*, **5**, 225.

17. Fukumura, K., Wakabayashi, S., Kataoka, N., Sakamoto, H., Suzuki, Y., Nakai, K., Mayeda, A. and Inoue, K. (2016) The exon junction complex controls the efficient and faithful splicing of a subset of transcripts involved in mitotic cell-cycle progression. *Int. J. Mol. Sci.*, **17**, 1153.

18. Fukumura, K., Inoue, K. and Mayeda, A. (2018) Splicing activator RNPS1 suppresses errors in pre-mRNA splicing: A key factor for mRNA quality control. *Biochem. Biophys. Res. Commun.*, **496**, 921–926.

19. Dominguez, D., Tsai, Y.H., Weatheritt, R., Wang, Y., Blencowe, B.J. and Wang, Z. (2016) An extensive program of periodic alternative splicing linked to cell cycle progression. *Elife*, **5**, e10288.

20. Fukumura, K., Yoshimoto, R., Sperotto, L., Kang, H.S., Hirose, T., Inoue, K., Sattler, M. and Mayeda, A. (2021) SPF45/RBM17-dependent, but not U2AF-dependent, splicing in a distinct subset of human short introns. *Nat. Commun.*, **12**, 4910.

21. Bolger, A.M., Lohse, M. and Usadel, B. (2014) Trimmomatic: a flexible trimmer for Illumina sequence data. *Bioinformatics*, **30**, 2114–2120.

22. Kim, D., Pertea, G., Trapnell, C., Pimentel, H., Kelley, R. and Salzberg, S.L. (2013) TopHat2: accurate alignment of transcriptomes in the presence of insertions, deletions and gene fusions. *Genome biology*, **14**, R36.

23. Trapnell, C., Hendrickson, D.G., Sauvageau, M., Goff, L., Rinn, J.L. and Pachter, L. (2013) Differential analysis of gene regulation at transcript resolution with RNA-seq. *Nat. Biotechnol.*, **31**, 46–53.

24. Katz, Y., Wang, E.T., Airoldi, E.M. and Burge, C.B. (2010) Analysis and design of RNA sequencing

experiments for identifying isoform regulation. *Nat. Methods*, **7**, 1009–1015.

25. Masuda, A., Takeda, J., Okuno, T., Okamoto, T., Ohkawara, B., Ito, M., Ishigaki, S., Sobue, G. and Ohno, K. (2015) Position-specific binding of FUS to nascent RNA regulates mRNA length. *Genes Dev.*, **29**, 1045–1057.

26. Honda, R., Korner, R. and Nigg, E.A. (2003) Exploring the functional interactions between Aurora B, INCENP, and survivin in mitosis. *Mol. Biol. Cell*, **14**, 3325–3341.

27. Badolato, J., Gardiner, E., Morrison, N. and Eisman, J. (1995) Identification and characterisation of a novel human RNA-binding protein. *Gene*, **166**, 323–327.

28. Gilberto, S. and Peter, M. (2017) Dynamic ubiquitin signaling in cell cycle regulation. *J. Cell Biol.*, **216**, 2259–2271.

29. Kwon, S.K., Kim, E.H. and Baek, K.H. (2017) RNPS1 is modulated by ubiquitin-specific protease 4. *FEBS Lett.*, **591**, 369–381.

30. Boehm, V., Britto-Borges, T., Steckelberg, A.L., Singh, K.K., Gerbracht, J.V., Gueney, E., Blazquez, L., Altmuller, J., Dieterich, C. and Gehring, N.H. (2018) Exon Junction Complexes Suppress Spurious Splice Sites to Safeguard Transcriptome Integrity. *Mol. Cell*, **72**, 482–495.

31. Blazquez, L., Emmett, W., Faraway, R., Pineda, J.M.B., Bajew, S., Gohr, A., Haberman, N., Sibley, C.R., Bradley, R.K., Irimia, M. *et al.* (2018) Exon Junction Complex Shapes the Transcriptome by Repressing Recursive Splicing. *Mol. Cell*, **72**, 496–509.

32. Ishigaki, Y., Nakamura, Y., Tatsuno, T., Hashimoto, M., Shimasaki, T., Iwabuchi, K. and Tomosugi, N. (2013) Depletion of RNA-binding protein RBM8A (Y14) causes cell cycle deficiency and apoptosis in human cells. *Exp. Biol. Med. (Maywood)*, **238**, 889–897.

33. Silver, D.L., Watkins-Chow, D.E., Schreck, K.C., Pierfelice, T.J., Larson, D.M., Burnetti, A.J., Liaw, H.J., Myung, K., Walsh, C.A., Gaiano, N. *et al.* (2010) The exon junction complex component Magoh controls brain size by regulating neural stem cell division. *Nat. Neurosci.*, **13**, 551–558.

34. Jang, S.W., Yang, S.J., Ehlen, A., Dong, S., Khoury, H., Chen, J., Persson, J.L. and Ye, K. (2008) Serine/arginine protein-specific kinase 2 promotes leukemia cell proliferation by phosphorylating acinus and regulating cyclin A1. *Cancer Res.*, **68**, 4559–4570.

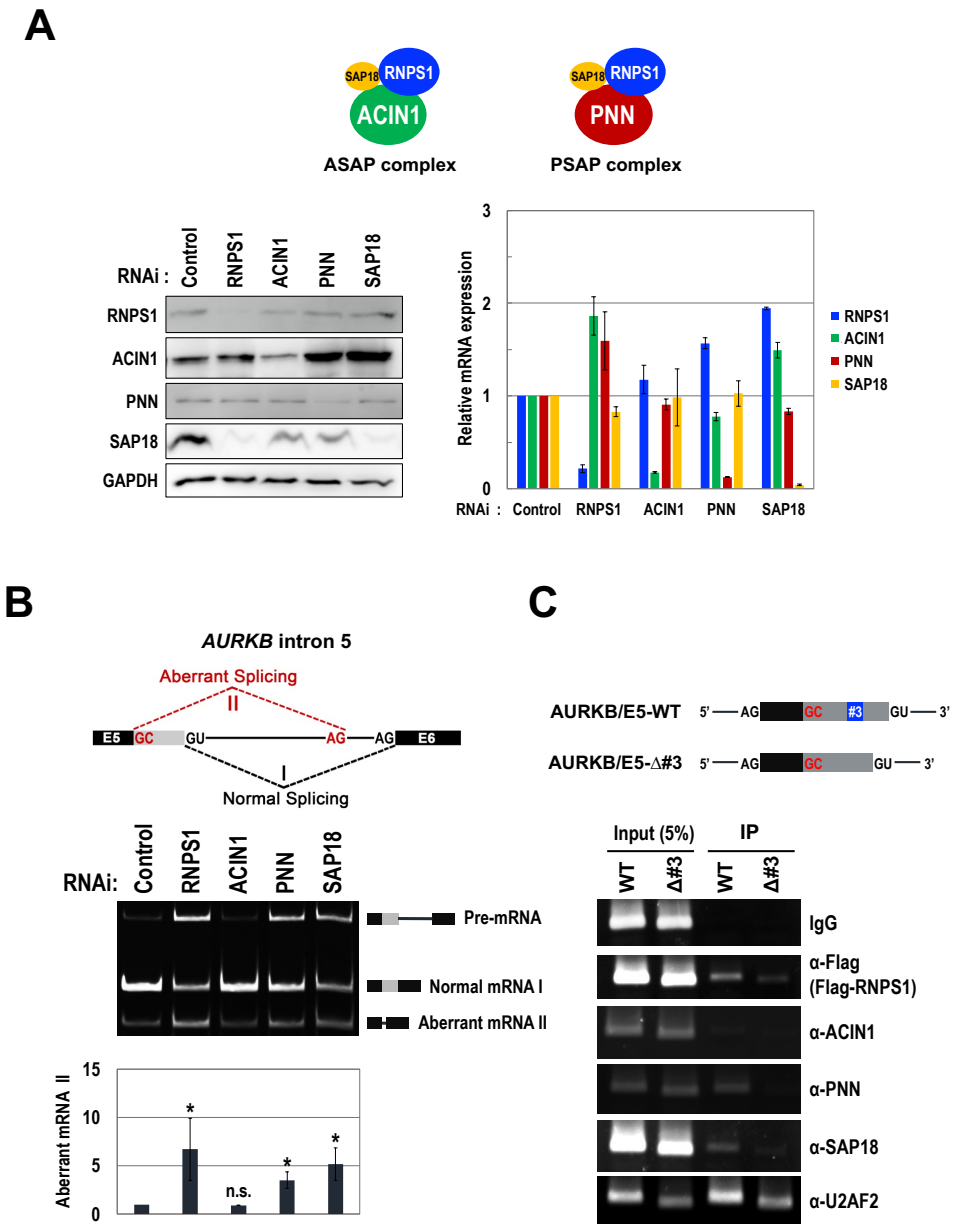

Figure 1. PSAP component binds to a specific site that is critical to prevent aberrant *AURKB* pre-mRNA splicing. (**A**) ASAP/PSAP components (RNPS1, ACIN1, PNN and SAP18) in HeLa cells were depleted by RNAi-mediated knockdown. These proteins were analyzed by Western blotting with indicated antibodies (left panel). These mRNA levels were analyzed by RT-qPCR using specific primer sets (right panel). Means ± standard errors (SE) are given. $^{*}P < 0.05$, $^{**}P < 0.005$, $^{***}P < 0.0005$, $^{n.s.}$(not statistically significant) $P>0.05$. (**B**) RNAi-mediated depletion of PSAP proteins induces aberrant splicing and intron 5 retention in *AURKB* pre-mRNA. Splicing products from the endogenous *AURKB* gene were detected by RT–PCR and visualized by PAGE. The bands on the PAGE gel were quantified. The ratios of the aberrantly spliced mRNA value (II) to the sum of the spliced mRNAs value (I+II) were standardized to that of the control siRNA and plotted. Means ± standard errors (SE) are given ($^{*}P < 0.05$, $^{n.s.}P>0.05$). (**C**) The PSAP, but not ASAP complex, binds to specific *cis*-element #3 in the *AURKB* exon 5. An RNA immunoprecipitation assay was performed using HeLa cells co-transfected with Flag-RNPS1 expression plasmids and the indicated AURKB-Exon 5 reporter mini-genes (WT or Δ#3). After Immunoprecipitation using the indicated antibodies, associated RNAs were detected by RT–PCR and visualized by agarose gel electrophoresis.

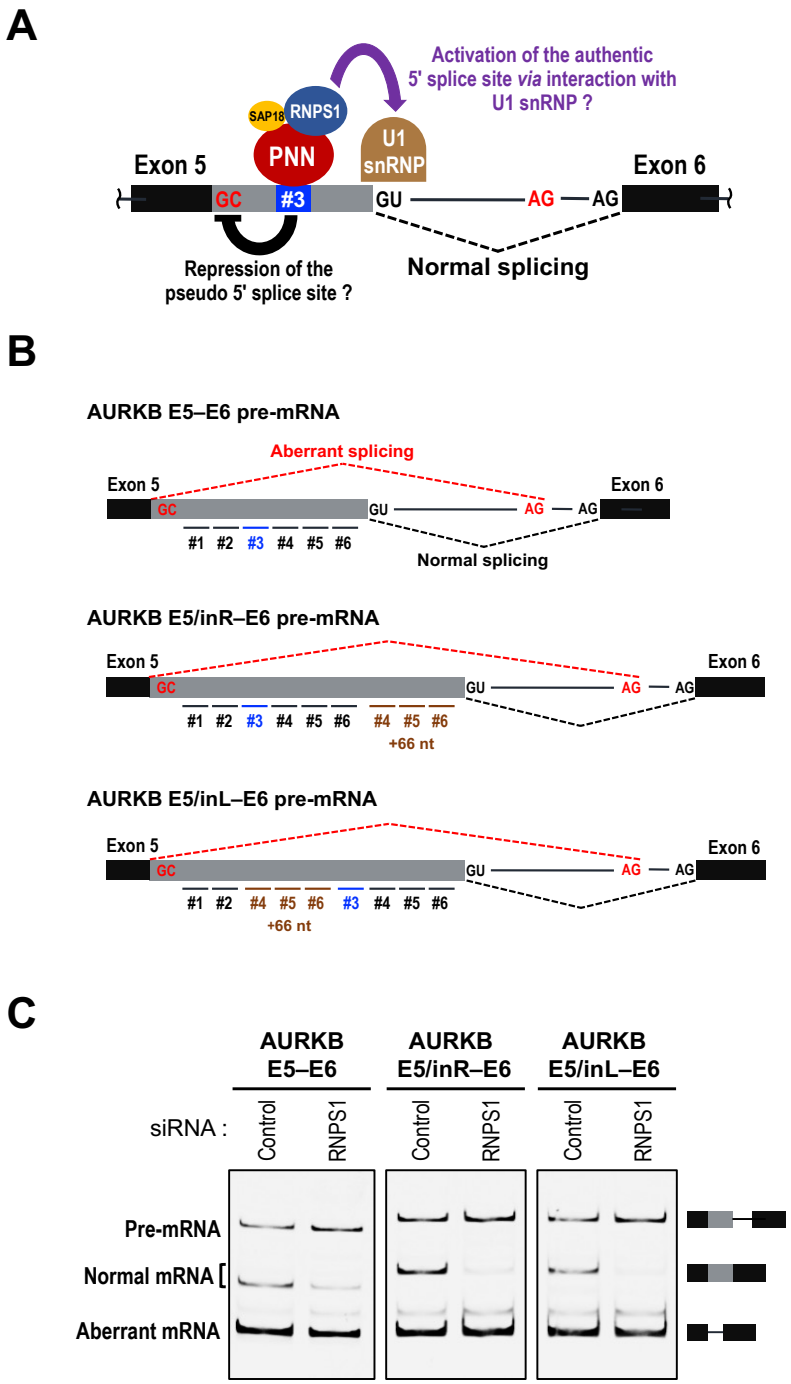

Figure 2. PSAP represses upstream pseudo 5' splice sites but not by direct masking. (**A**) Schematic diagram of two possible PSAP-mediated mechanisms to maintain normal splicing. (i) PSAP on the target site (#3) can activate the downstream authentic 5' splice site through RNPS1 interaction with LUC7L3 in U1 snRNP [18]. (ii) PSAP on the target site (#3) can repress the upstream pseudo 5' splice site through either direct masking or indirect interference. (**B**) Three *AURKB* mini-gene transcripts to test the above models. The distances from PSAP-binding site (#4) to either upstream authentic 5' splice site or downstream pseudo 5' splice site were expanded by inserted duplicated fragment (#4-#5-#6); i.e., E5/inR–E6 and E5/inL–E6, respectively. (**C**) *In cellulo* splicing assay of ectopically expressed three *AURKB* mini-genes described in (B). Splicing products were detected by RT–PCR using specific primer sets and visualized by PAGE. Normal and aberrant mRNA products, depicted in (B), are shown schematically at the right side.

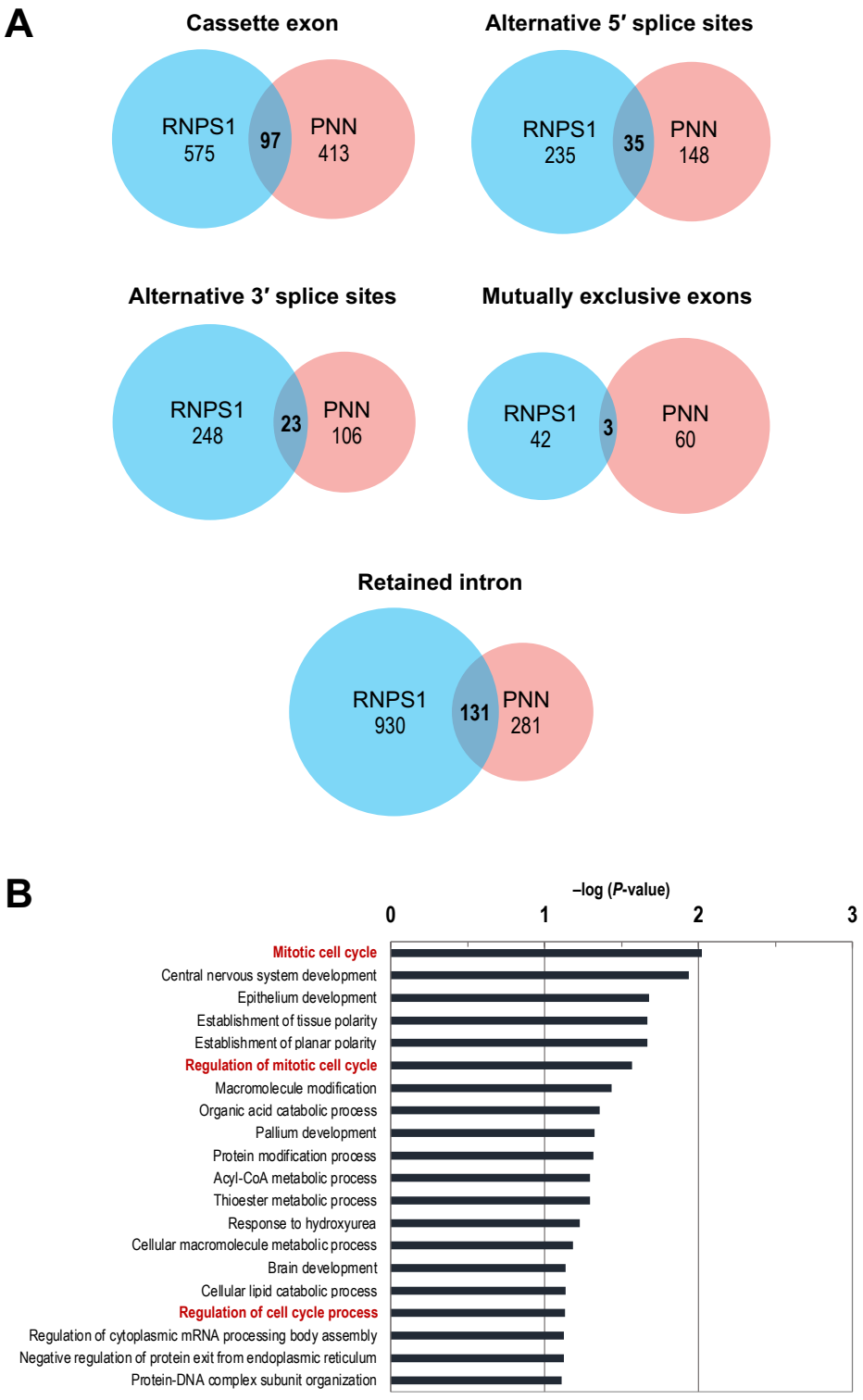

Figure 3. PSAP often regulates alternative splicing of genes involved in mitotic cell cycle progression. (**A**) RNA-Seq analyses of RNPS1- and PNN-knockdown HEK293 cells. The number of statistically significant changes in each alternative splicing pattern is visualized as Venn diagram. (**B**) Gene ontology analysis for genes associated with overlapping splicing changes (total 289) in the RNPS1- and PNN-deficient HEK293 cells. The PSAP-dependent changes of alternative splicing are significantly enriched in genes involved in cell cycle processes (highlighted in dark red).

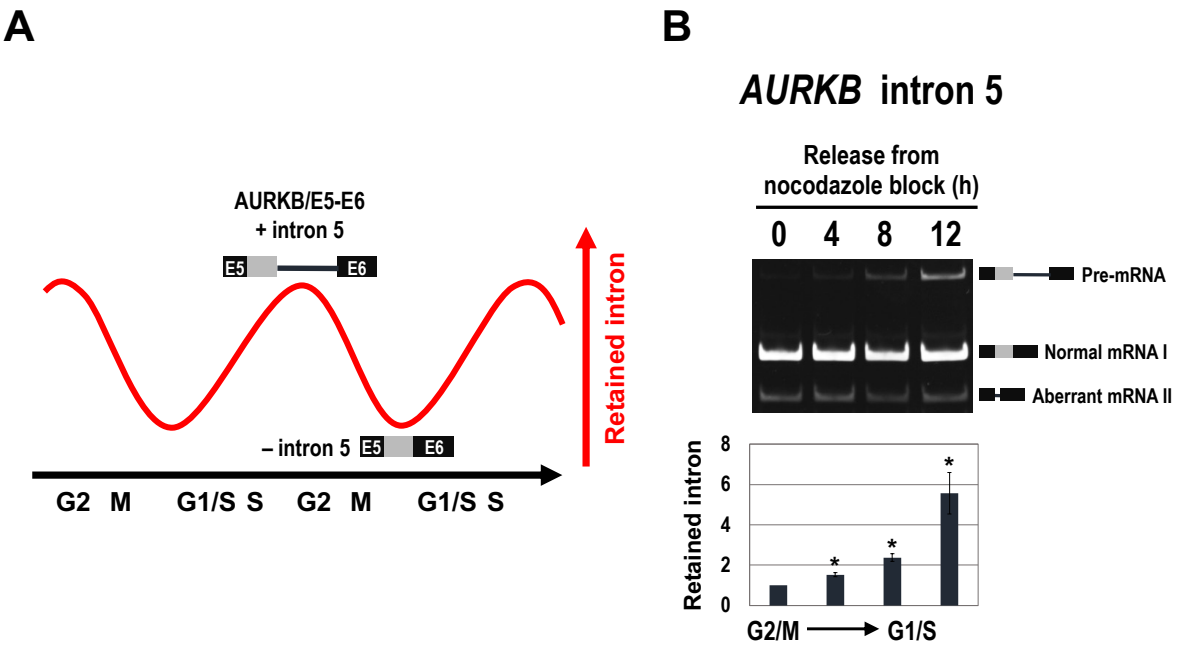

Figure 4. Cyclical intron 5 retention of *AURKB* pre-mRNA during the cell cycle. (**A**) Schematic representation of cyclical retention of *AURKB* intron 5 (modified from 19). (**B**) Periodic *AURKB* intron 5 retention across the cell cycle is recapitulated in our experimental system. HEK293 cells were synchronized in G2/M phase by treating with nocodazole, washed, released, and harvested at the indicating time points. The splicing of *AURKB* intron 5 was analyzed by RT–PCR followed by PAGE (upper gel), and the retained intron product was quantitated by RT–qPCR (lower graph). The retained intron product value was standardized to that at the start time (0 h). A trace level of aberrantly spliced product (II), which was not changed across the cell cycle, was due to the toxicity of nocodazole. Means ± SE are given (*$P < 0.05$).

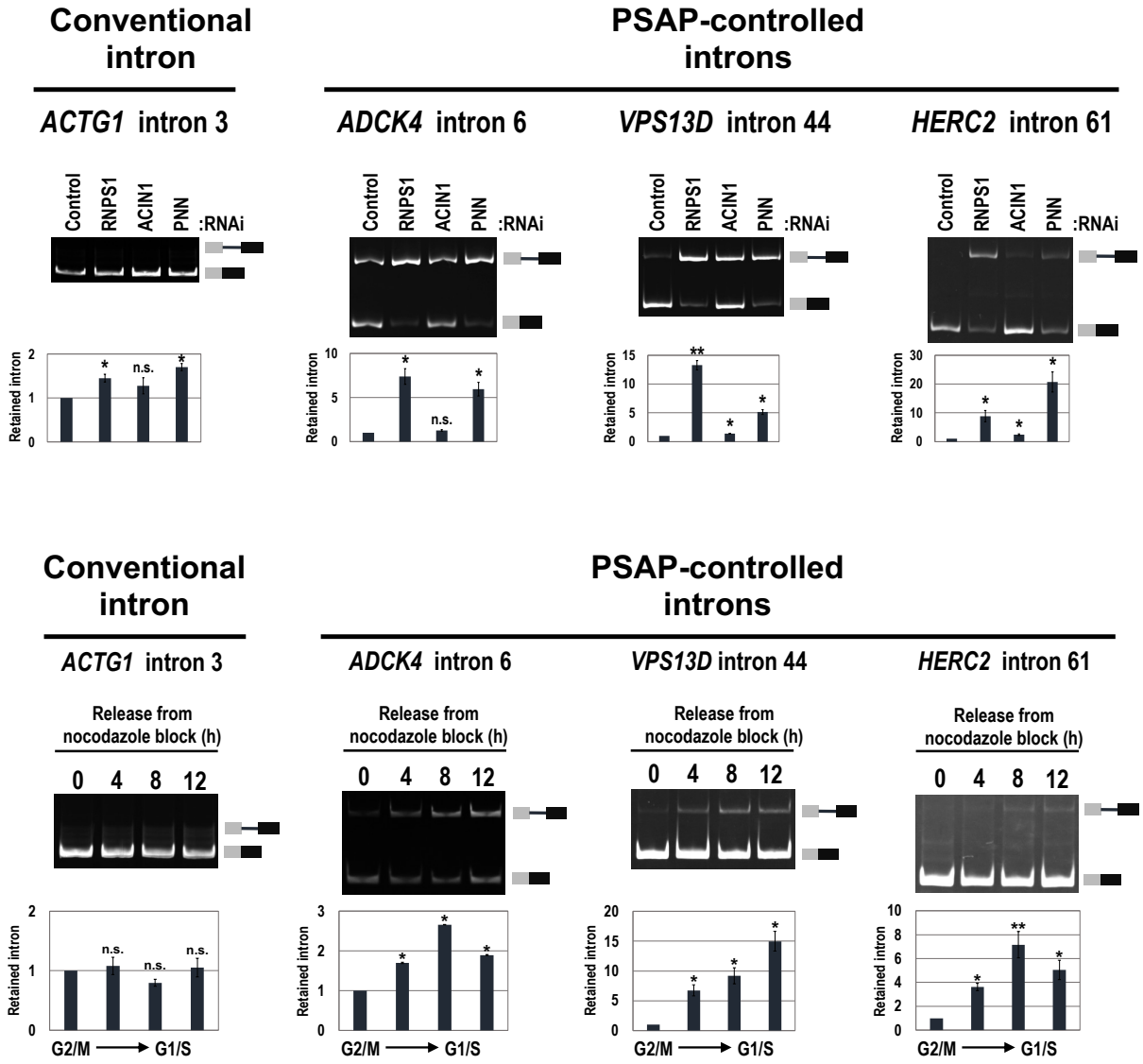

Figure 5. PSAP modulates cyclical intron retention during the cell cycle. (**A)** Three representative introns (*ADCK4* intron 6, *VPS13D* intron 44, *HERC2* intron 61) selected from RNA-Seq data were validated by RNAi-mediated knockdown in HEK293 cells. Endogenous splicing in these introns together with a control intron (*ACTG1* intron 3) was analyzed by RT–PCR followed by PAGE (upper gel), and the retained intron product was quantitated by RT–qPCR (lower graph). Means ± SE are given (*P < 0.05, **P < 0.005, $^{n.s.}$ P>0.05). (**B**) Periodic intron retention across the cell cycle was observed in these three PSAP-regulated introns (*ADCK4* intron 6, *VPS13D* intron 44, *HERC2* intron 61). HEK293 cells were synchronized in G2/M phase by nocodazole and released. Endogenous splicing in these introns together with control intron (*ACTG1* intron 3) was analyzed (upper gel) and quantitated (lower graph) as described in (C). Means ± SE are given (**P* < 0.05, ***P* < 0.005, $^{n.s.}$ *P* > 0.05).

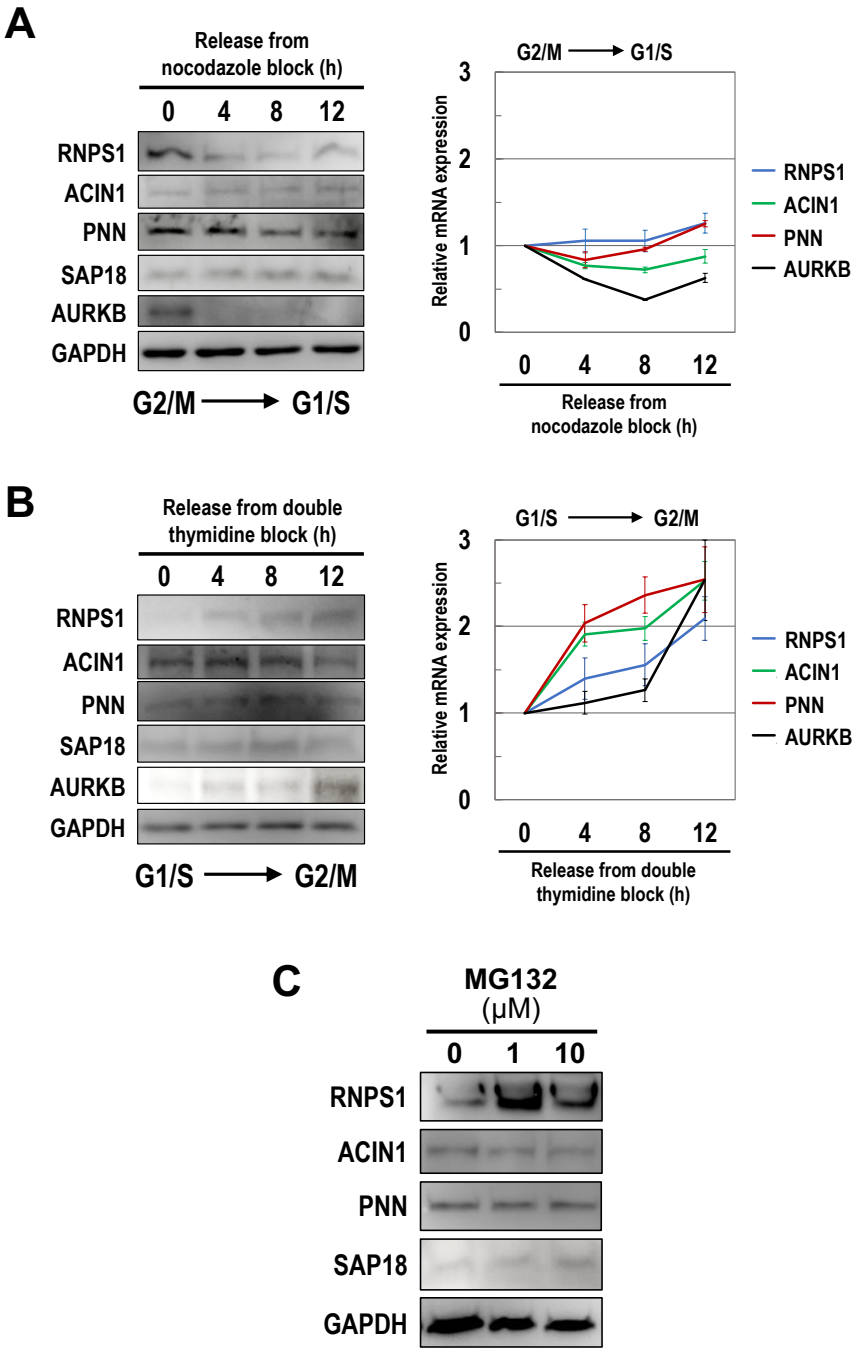

Figure 6. RNPS1 protein level is modulated during the cell cycle exclusively by the ubiquitin-proteasome pathway. (**A**) Expression level of RNPS1, but not all other ASAP and PSAP proteins, decreases from G2/M to G1/S phase. HEK293 cells were synchronized in G2/M phase by nocodazole and released cells were harvested at indicated time points. Total proteins and RNAs were analyzed by Western blotting with indicated antibodies (left panel) and RT–qPCR (right panel), respectively. (**B**) Expression level of RNPS1, but not all other ASAP and PSAP components, increases from G1/S to G2/M phase. HEK293 cells were synchronized at G1/S phase by double thymidine block and total proteins and RNAs were analyzed as described in (A). (**C**) The protein levels of PSAP components (RNPS1, PNN and SAP18) in the presence of proteasome inhibitor MG132. A common solvent, dimethyl sulfoxide (DMSO), was added in 0 μM. HeLa cells were cultured for 24 h with the indicated concentration of MG132 and the protein levels were analyzed by Western blotting using the antibody against each protein.

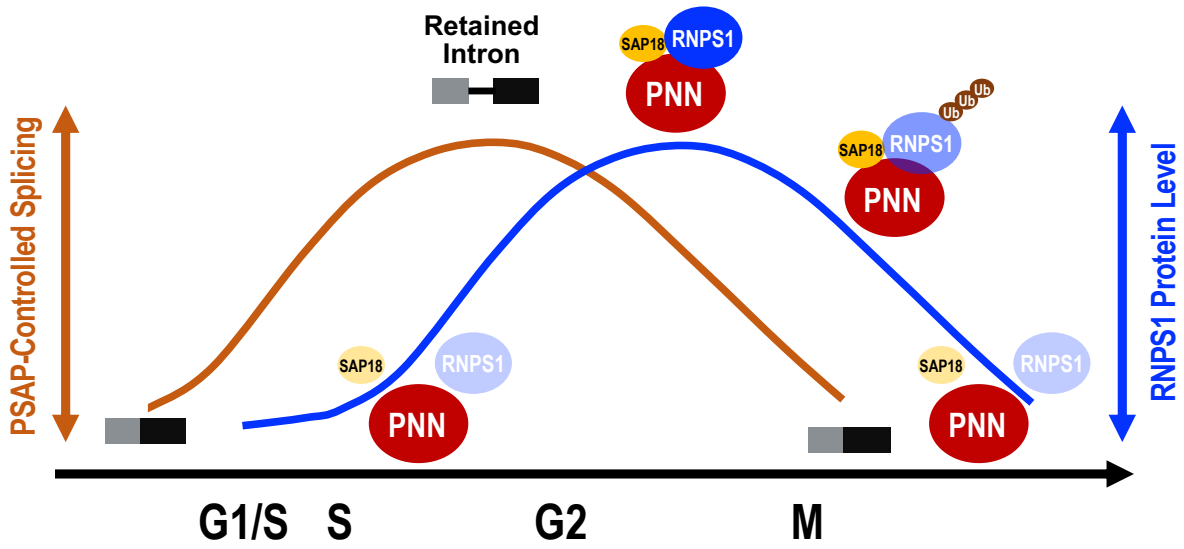

Figure 7. The model of periodic modulation of splicing during cell cycle progression that is regulated by RNPS1 component in PSAP. We discovered that RNPS1 protein, but neither PNN nor SAP18, in PSAP plays an essential role to control periodical splicing during the cell cycle.

RNPS1 in PSAP complex controls cyclical pre-mRNA splicing over the cell cycle

Kazuhiro Fukumura[1,*], Akio Masuda[2], Jun-ichi Takeda[2], Kinji Ohno[2] and Akila Mayeda[1,*]

[1]Division of Gene Expression Mechanism, Center for Medical Science, Fujita Health University, Toyoake, Aichi 470-1192, Japan
[2]Division of Neurogenetics, Center for Neurological Disease and Cancer, Nagoya University Graduate School of Medicine, Nagoya, Aichi 466-8550, Japan

*To whom Correspondences should be addressed. Tel: +81 562 93 9378; Email: fukumura@fujita-hu.ac.jp (K.F.). Tel: +81 562 93 9377; Email: mayeda@fujita-hu.ac.jp (A.M.)

Contents

Table S1

Figure S1

Figure S2

Figure S3

SUPPLEMENTARY REFERENCES

Tables S2, S3, S4
(Uploaded in the separate Excel files)

Table S1 List of all the synthetic oligonucleotides used in the experiments

siRNAs (sense sequences) for cellular knockdown (*T*: deoxyribonucleotide)		
RNPS1-siRNA	5′-GCAAAGACCGCUCAGAUGA*TT*-3′	Knockdown of *RNPS1*
ACIN1-siRNA	5′-GAGGCCUUCUGGAUUGACA*TT*-3′	Knockdown of *ACIN1*
PNN-siRNA	5′-GAAGGUAGACGCAUCGAAU*TT*-3′	Knockdown of *PNN*
SAP18-siRNA	5′-CCAGCGAGUUGCAGAUCUA*TT*-3′	Knockdown of *SAP18*
GPATCH8-siRNA	5′-GACCAGAGCUGCUAUAGUA*TT*-3′	Knockdown of *GPATCH8*
LUC7L3-siRNA	5′-GAAGUAGAACGUAGGAUCA*TT*-3′	Knockdown of *LUC7L3*
Primer DNAs for plasmid constructions		
AURKB/I4-E5-I5-F	5′-CAGTGTGCTGGAATTGTTCTGAGTTGCCTTCCTC-3′	Construction of pcDNA3-AURKB/E5-WT & pcDNA3-AURKB/E5-Δ#3
AURKB/I4-E5-I5-R	5′-TAGATGCATGCTCGAGGCTTCGGCTCAGGGGGC-3′	
AURKB/E5/inR-E6-F1	5′-GAAATCCAGGCCCACAAGTCCCAGATAGAG-3′	Construction of pcDNA3-AURKB/E5/inR-E6
AURKB/E5/inR-E6-R1	5′-CAACCCATACTGCAGGTGGGCCTGGATTTC-3′	
AURKB/E5/inR-E6-F2	5′-GAAATCCAGGCCCACCTGCAGTATGGGTTG-3′	
AURKB/E5/inR-E6-R2	5′-CTCTATCTGGGACTTGTGGGCCTGGATTTC-3′	
AURKB/E5/inL-E6-F1	5′-AAGAAAAGCCATTTCATAAGTCCCAGATAGAGAA-3′	Construction of pcDNA3-AURKB/E5/inL-E6
AURKB/E5/inL-E6-R1	5′-GGACCTTGAGCGCCACGGTGGGCCTGGATTTCGA-3′	
AURKB/E5/inL-E6-F2	5′-TCGAAATCCAGGCCCACCGTGGCGCTCAAGGTCC-3′	
AURKB/E5/inL-E6-R2	5′-TTCTCTATCTGGGACTTATGAAATGGCTTTTCTT-3′	
Primer DNAs for assays		
AURKB/E5-F	5′-GGAATTCCGGCGGCACTTCACAATTGATG-3′	Splicing assay of endogenous *AURKB* intron 5
AURKB/E6-R	5′-CCGCTCGAGGCTGTTCGCTGCTCGTCAA-3′	
MDM2/E8-F	5′-CTTTGATGAAAGCCTGGCTC-3′	Splicing assay of endogenous *MDM2* intron 9
MDM2/E10-R	5′-CCTGCCTGATACACAGTAACT-3′	
RNPS1-PCR-F	5′-GAAGCACATGGATGGAGGAC-3′	PCR & qPCR detections of endogenous *RNPS1* mRNA
RNPS1-PCR-R	5′-GGAGACCTGCGCCACATA-3′	
ACIN1-PCR-F	5′-GCAGACCAAGTCAGCAATGA-3′	PCR & qPCR detections of endogenous *ACIN1* mRNA
ACIN1-PCR-R	5′-CCCCCTCTGTGTCACTGTTT-3′	
PNN-PCR-F	5′-AGAAGAGAATCACGCCAGGA-3′	PCR & qPCR detections of endogenous *PNN* mRNA
PNN-PCR-R	5′-CCGCTTTTGCCTTTCAGTAG-3′	
SAP18-PCR-F	5′-ATGCTCGCTGCAGGGGTC-3′	qPCR detection of endogenous *SAP18* mRNA
SAP18-PCR-R	5′-TTAATATGGTCTCATGCGCCCT-3′	
GPATCH8-PCR-F	5′-CTTCAGGGTCTGCCTGTAGC-3′	PCR detection of endogenous *GPATCH8* mRNA
GPATCH8-PCR-R	5′-GTTTTCGTTTCTTGCGCTTC-3′	

LUC7L3-PCR-F	5′-CTCAAGCCGAACATCAGACA-3′	PCR detection of endogenous *LUC7L3* mRNA
LUC7L3-PCR-R	5′-CTCTGTCCCGACTTTTGCTC-3′	
ACTG1-PCR-F	5′-CCCATCTACGAGGGCTACG-3′	PCR & qPCR detections of endogenous *ACTG1* mRNA
ACTG1-PCR-R	5′-TTCATGAGGTAGTCGGTCAGG-3′	
AURKB-PCR-F	5′-CTCCTACCCCTGGCCCTA-3′	qPCR detection of endogenous *AURKB* mRNA
AURKB-PCR-R	5′-GATGGGGTGACAGGCTCTT-3′	
T7	5′-AATACGACTCACTATAG-3′	RIP assay for *AURKB*/E5-WT and *AURKB*/E5Δ#3 reporter
AURKB/E6-R	5′-CCGCTCGAGGCTGTTCGCTGCTCGTCAA-3′	
ACTG1/E3-F	5′-TGACCCTGAAGTACCCCATT-3′	Splicing assay of endogenous *ACTG1* intron 3
ACTG1/E4-R	5′-TGGTGGTGAAGCTGTAGCCT-3′	
ADCK4/E6-F	5′-AATGCCGAGCGGATTGTG-3′	Splicing assay of endogenous *ADCK4* intron 6
ADCK/E7-R	5′-GGACCCGCTCAAAGATGTG-3′	
VPS13D/E44-F	5′-TCTCTTCACTCCCACCAGTG-3′	Splicing assay of endogenous *VPS13D* intron 44
VPS13D/E45-R	5′-GTGTCCATAGAGTGGCACTCT-3′	
HERC2/E61-F	5′-ACTGTGACAAACCAAGGCTG-3′	Splicing assay of endogenous *HERC2* intron 61
HERC2/E62-R	5′-CTTCATCGGTCAGAGCCAG-3′	
AURKB/spliced-F	5′-CAGGCCCACCTGCACCAT-3′	qPCR detection of endogenous *AURKB* spliced mRNA
AURKB/E6-R	5′-CCGCTCGAGGCTGTTCGCTGCTCGTCAA-3′	
AURKB/I5-F	5′-AGTGAGCCCCTTTAGCTCTT-3′	qPCR detection of endogenous *AURKB* intron 5 retained mRNA
AURKB/I5-R	5′-TGGGAGTGGTAAGGGGAAA-3′	
ADCK4/spliced-F	5′-AGATGCTCAGCATCCAGGAC-3′	qPCR detection of endogenous *ADCK4* spliced mRNA
ADCK4/E7-R	5′-GGACCCGCTCAAAGATGTG-3′	
ADCK4/E6-F	5′-AATGCCGAGCGGATTGTG-3′	qPCR detection of endogenous *ADCK4* intron 6 retained mRNA
ADCK4/I6-R	5′-GAGTCGAGGGTCATGCTGTA-3′	
VPS13D/spliced-F	5′-ATCAGCTCCAGACAAGCCAG-3′	qPCR detection of endogenous *VPS13D* spliced mRNA
VPS13D/E45-R	5′-GTGTCCATAGAGTGGCACTCT-3′	
VPS13D/I44-F	5′-GAGGACCATTGCCTGAAAGTG-3′	qPCR detection of endogenous *VPS13D* intron 44 retained mRNA
VPS13D/E45-R	5′-GTGTCCATAGAGTGGCACTCT-3′	
HERC2/E61-F	5′-ACTGTGACAAACCAAGGCTG-3′	qPCR detection of endogenous *HERC2* spliced mRNA
HERC2/spliced-R	5′-GACCGAGAAGGACTTTCACCA-3′	
HERC2/I61-F	5′-TGCCTGTGCGTGATTCTG-3′	qPCR detection of endogenous *HERC2* intron 61 retained mRNA
HERC2/E62-R	5′-CTTCATCGGTCAGAGCCAG-3′	

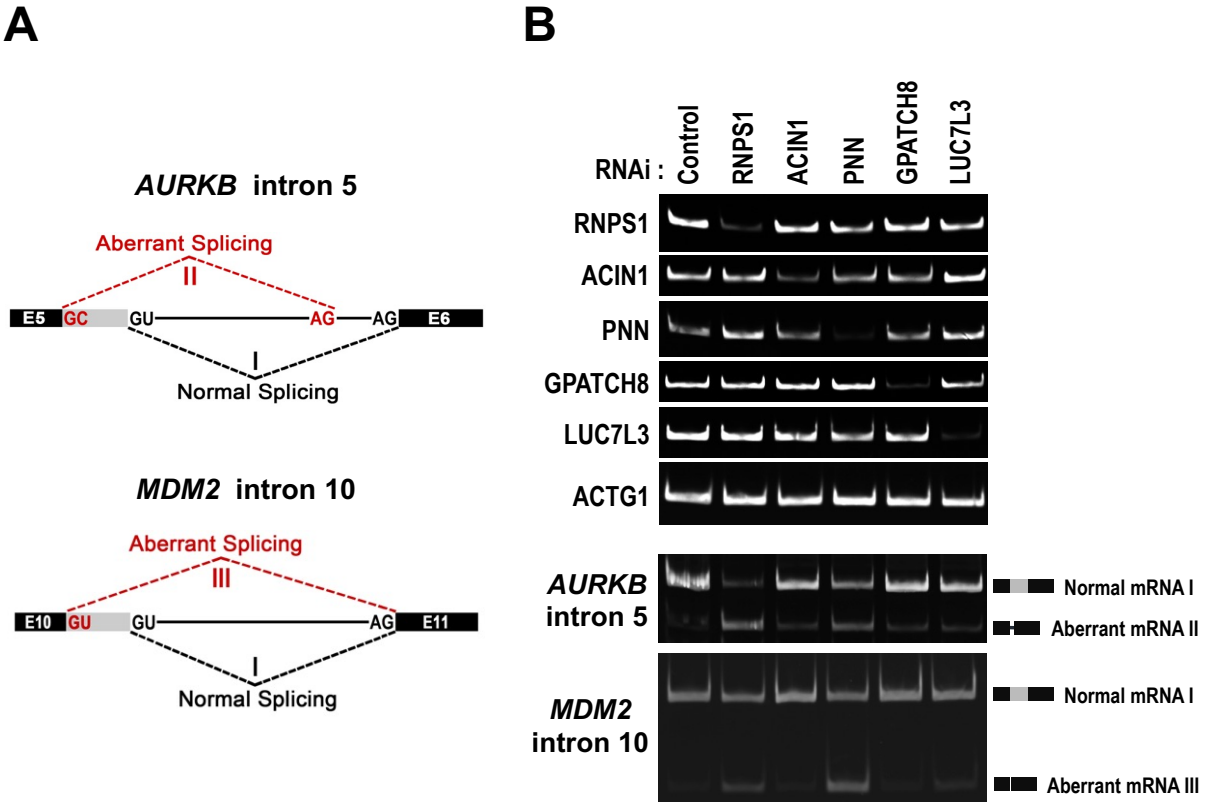

Figure S1. Knockdown of PSAP-specific component (PNN), but not ASAP-specific component (ACIN1) and other RNPS1-binding factors (GPATCH8 and LUC7L3), induces aberrant splicing in the *AURKB* and *MDM2* pre-mRNAs. (**A**) Schematic diagram of pre-mRNA splicing pathways that genefrate the normal mRNA (I) and aberrant mRNAs (II, III) in the *AURKB* intron 5 and *MDM2* intron 10. Previously it was shown that the aberrant mRNAs (II, III) of these distinct pre-mRNAs are generated by RNAi-mediated depletion of RNPS1, a component of PSAP (1). (**B**) RNAi-mediated depletion of the ASAP-specific component (ACIN1) and PSAP-specific component (PNN) together with other RNPS1-binding proteins (GTATCH8 and LUC7L3) in HeLa cells and these proteins were analyzed by Western blotting with indicated antibodies (upper panel). Indicated spliced mRNAs (I, II, III) from the endogenous *AURKB* and *MDM2* genes were detected by RT–PCR and visualized by PAGE (lower panel). GPATCH8 (G patch domain-containing protein 8) was isolated from human brain cDNA library and function was unknown. Previous exome sequencing study showed that a mutation in GPATCH8 associated with hyperuricemia co-segregating with osteogenesis imperfecta (2). LUC7L3 (LUC7 like3) is a homolog of yeast U1 snRNP component LUC7, which is involved in alternative splicing regulation in human (3,4).

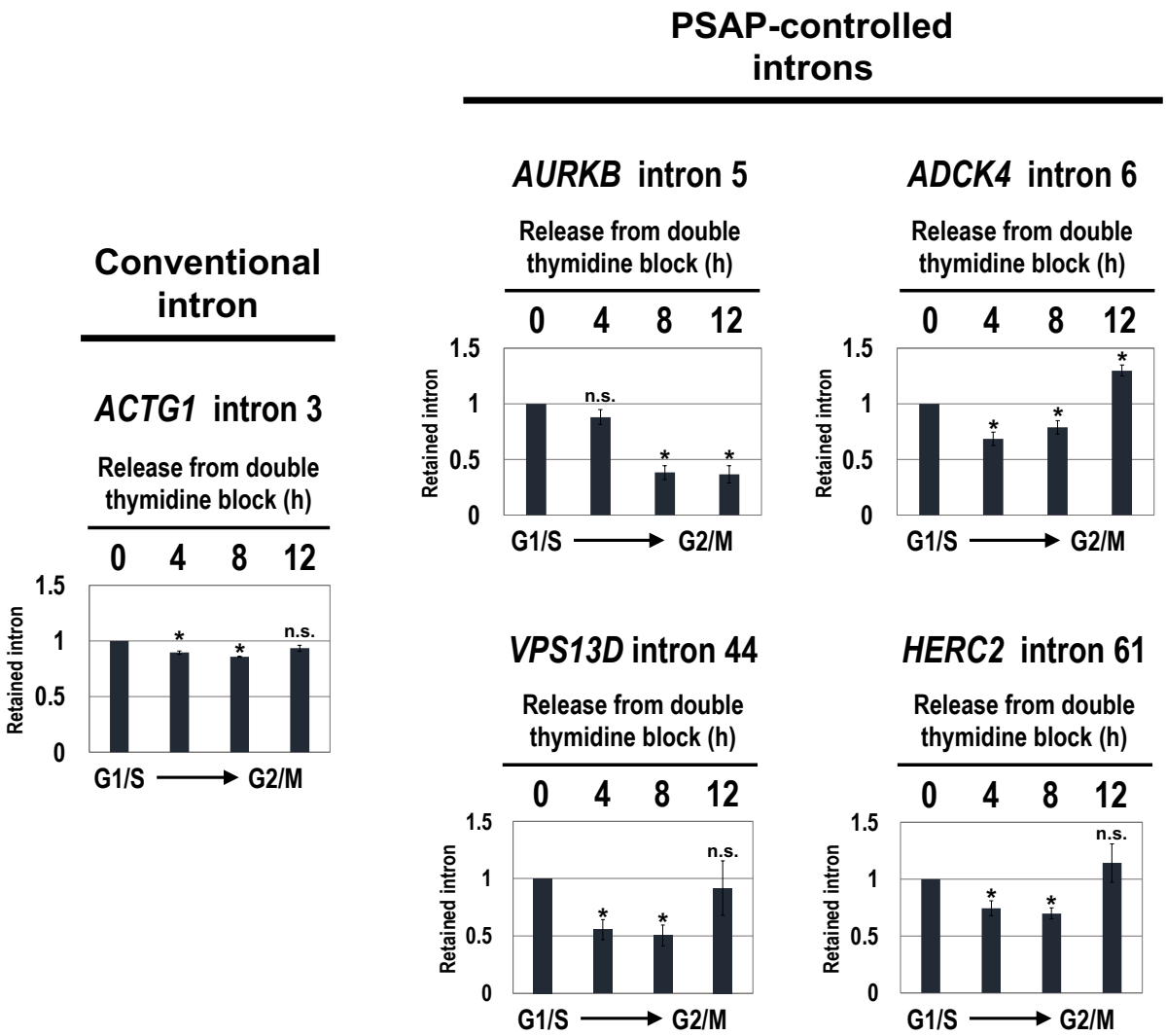

Figure S2. PSAP modulates periodic intron retention events across the cell cycle. HEK293 cells were synchronized in G1/S phase by double thymidine block, released, and harvested at the indicating time points. Endogenous splicing in the indicated introns was analyzed by RT–qPCR. Means ± SE are given (*$P < 0.05$, **$P < 0.005$, $^{n.s.}$ $P > 0.05$).

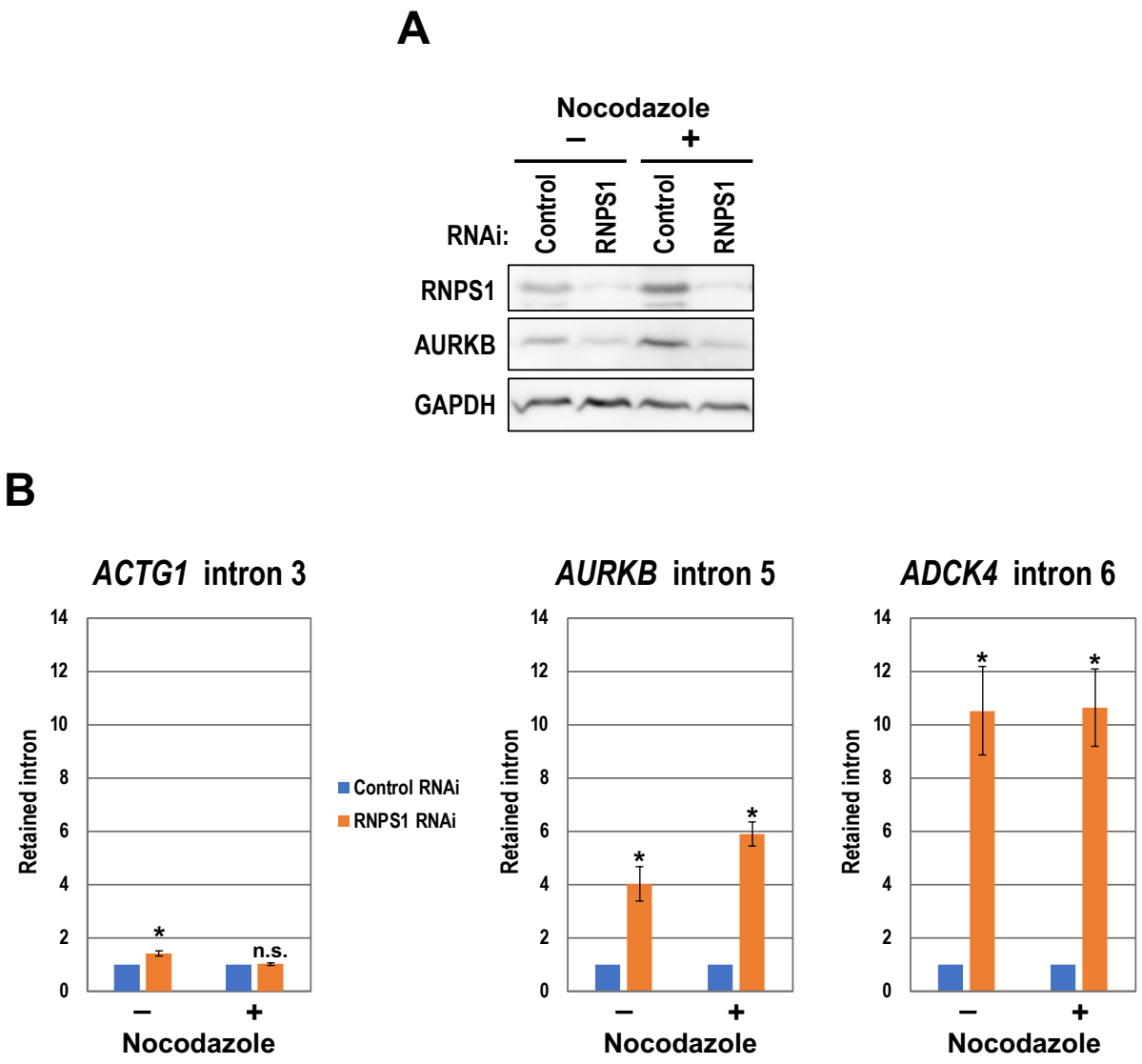

Figure S3. Knockdown of RNPS1 induces retention of PSAP-regulated introns irrespective of cell cycle phase. (**A**) RNPS1 was depleted by RNAi-mediated knockdown in HEK293 cells and treated with nocodazole to arrest the cell cycle at the G2/M phase. Proteins were analyzed by Western blotting with indicated antibodies. *AURKB* is downregulated by RNPS1-knockdown as previously described (1). *CCNB1*, encoding cyclin B1, regulates cell cycle. (B) Indicated retained introns were analyzed by RT–qPCR and the values were standardized to that of the control-knockdown and plotted. Means ± SE are given (*$P < 0.05$, $^{n.s.}$ $P > 0.05$).

SUPPLEMENTARY REFERENCES

1. Fukumura, K., Inoue, K. and Mayeda, A. (2018) Splicing activator RNPS1 suppresses errors in pre-mRNA splicing: A key factor for mRNA quality control. *Biochem. Biophys. Res. Commun.*, **496**, 921–926.

2. Kaneko, H., Kitoh, H., Matsuura, T., Masuda, A., Ito, M., Mottes, M., Rauch, F., Ishiguro, N. and Ohno, K. (2011) Hyperuricemia cosegregating with osteogenesis imperfecta is associated with a mutation in GPATCH8. *Hum. Genet.*, **130**, 671–683.

3. Fortes, P., Bilbao-Cortes, D., Fornerod, M., Rigaut, G., Raymond, W., Seraphin, B. and Mattaj, I.W. (1999) Luc7p, a novel yeast U1 snRNP protein with a role in 5' splice site recognition. *Genes Dev.*, **13**, 2425–2438.

4. Gao, G., Xie, A., Huang, S.C., Zhou, A., Zhang, J., Herman, A.M., Ghassemzadeh, S., Jeong, E.M., Kasturirangan, S., Raicu, M. *et al.* (2011) Role of RBM25/LUC7L3 in abnormal cardiac sodium channel splicing regulation in human heart failure. *Circulation*, **124**, 1124–1131.